Journal of Engineering Science and Technology
Vol. 18, No. 1 (2023) 653 - 670
© School of Engineering, Taylor's University

REMOVAL OF CURCUMIN DYES FROM AQUEOUS SOLUTIONS USING CARBON MICROPARTICLES FROM JACKFRUIT SEEDS BY BATCH ADSORPTION EXPERIMENT

ASEP BAYU DANI NANDIYANTO*, MELI FIANDINI, RISTI RAGADHITA, RINA MARYANTI, DWI FITRIA AL HUSAENI, DWI NOVIA AL HUSAENI

Universitas Pendidikan Indonesia, Jl Setiabudhi No. 229, Bandung Indonesia
*Corresponding Author: nandiyanto@upi.edu

Abstract

The purpose of this study was to examine the removal of dye from curcumin in an aqueous solution using carbon microparticles from jackfruit seeds via a batch adsorption experiment and their adsorption isotherm characteristics. The fabrication of carbon microparticles was prepared in several steps: (1) separating the seeds from jackfruit (2) washing jackfruit seeds, (3) carbonization of jackfruit seeds at 230°C for 7 hours, (4) saw-milling process to obtain carbon particles, and (5) sieve analysis to obtain the specific size of carbon. To find out what happened to the adsorption process, we compared the adsorption results with 10 standard isotherm models, including Langmuir, Freundlich, Temkin, Dubinin-Radushkevich, Fowler-Guggenheim, Hill-Deboer, Jovanovic, Harkin-Jura, Flory-Huggins, and Halsey. In addition, carbon characterization was also carried out using an optical microscope and Fourier transform infrared (FTIR) analysis. The results revealed that several models, namely Jovanovic (R^2 = 0.9383), Langmuir (R^2 = 0.9159), Freundlich (R^2 = 0.8509), and Halsey (R^2 = 0.8509) are suitable for representing the adsorption equilibrium with coefficient correlation (R^2) is close to 1. The adsorption capacity of carbon from jackfruit seeds is 909.0909 mg/g. This study's overall conclusion is that the adsorption process is monolayer, endothermic, profitable, and non-spontaneous. According to the findings, alternative carbon microparticles fabricated from jackfruit seeds can be used as an adsorbent to treat dye waste.

Keywords: Adsorption, Carbon, Curcumin, Isotherm adsorption, Jackfruit seeds.

1. Introduction

Wastewater is residual water originating from household and industrial waste (i.e. paint, electroplating, cement, mining, dyeing, etc) which generally contains substances that are harmful to human health and the environment [1, 2]. Dye waste from the textile industry ranks first in freshwater pollution [3]. The discharge of dye waste directly into rivers has disastrous consequences for flora and aquatic fauna. In addition, dye waste can also seep into and contaminate groundwater [4, 5]. Several physical and chemical methods, such as coagulation, electro-coagulation, flocculation, filtration, membrane separation, reverse osmosis adsorption, precipitation, and bioremediation have been used to remove dyes from wastewater [6-8]. However, these methods are expensive, complex, ineffective, and easy to cause secondary pollution [9].

Adsorption is an easy waste treatment method that can be used to treat dye waste [10]. This is due to the cost-effective adsorption method for removing dyes, especially at low concentrations and using small amounts of chemicals [11, 12]. In the adsorption process, an adsorbent is used where the dye is adsorbed on the surface and settles so that clean water is obtained above the batch [13]. The adsorbent commonly used is carbon. Carbon can be sourced from organic and inorganic materials [14]. Carbon from organic matter comes from animals, plants (cellulose, hemicellulose, lignin, etc.), and agricultural waste (rock, shells, skins, bagasse, vegetables, rice husk, fruit seeds, etc.). While carbon from inorganic materials comes such as limestone, dolomite, carbon dioxide, and marble [15, 16].

In recent years, many researchers have used agricultural waste materials as adsorbents because they are cheap, affordable, and easy to obtain to produce carbon [17]. In addition, many researchers have succeeded in using adsorbents from agricultural waste which can be seen in Table 1.

Table 1. Example of the current reports on the fabrication of adsorbents from agricultural waste and their isotherm adsorption.

No.	Source of agricultural waste	Type of Adsorbent	Results	Ref.
1.	Rice Husk	Carbon	The carbon prepared from rice husk has an agglomeration and porous structure. Thus, the absorption efficiency is good.	[18]
2.	Red Dragon	Carbon	The best characteristic of the adsorption isotherm for use with dragon fruit peel waste as an adsorbent is the Dubinin-Radushkevich isotherm model.	[19]
3.	Pineapple Peel	Carbon	The adsorbent from pineapple peel waste follows the Freundlich model with a multilayer adsorption type on heterogeneous surfaces.	[20]
4.	Banana Stem	Carbon	The type of physical interaction carbon adsorption derived from banana stems is very good and has the potential to be used as an adsorbent.	[21]
5.	Rice Straw	Carbon	Carbon preparation of rice straw makes porous carbon particles effective and the change in porosity has a direct impact on the ability of the product to absorb molecules.	[22]
6.	Rice Straw	Carbon	Based on the findings, adsorption on the surface of pumpkin carbon microparticles occurred as a monolayer with physical phenomena.	[23]

No.	Source of agricultural waste	Type of Adsorbent	Results	Ref.
7.	Pumpkin	Carbon	The size of particles has a direct impact on the adsorption process. The absorption of soursop fruit peel waste material occurs on a multi-layered surface and physical interactions occur between adsorbent adsorbate.	[24
8.	Soursop Peel Waste	Carbon	Based on results, bio-adsorbent peanut peel can adopt metal ions (lead, copper, zinc, and cadmium) with the order of adsorption ability carried out was lead > zinc > copper > cadmium.	[25]
9.	Peanut Peel	Carbon	Adsorption on the surface of Chinese Herbal has great potential to remove ammonium phosphate from wastewater.	[26]
10.	Chinese Herbal (*Pleurotus ostreatus*)	Carbon	The adsorption capacity of potato peel at 107.2 mg/L following the Langmuir isotherm revealed that the adsorption mechanism was chemisorption.	[27]
11.	Potato Peel	Carbon	The kinetics and isotherm models were evaluated showing that the Langmuir isotherm with pseudo-order monolayer is the most suitable.	[28]
12.	Bagasse	Carbon	The adsorbent-derived tapioca peel succeeded in removing organic dyes. Based on the analysis, the adsorption isotherm follows the Freundlich isotherm model with pseudo-second-order kinetics.	[29]
13.	Tapioca Peel	Carbon	Freundlich isotherm model is the most appropriate adsorption isotherm model with Jujube Seeds Waste as an adsorbent.	[30]
14.	Jujube Seeds	Carbon	Solid soya is very suitable and well-used as an adsorbent to remove lead (II) ions.	[31]
15.	Oiled Soya	Carbon	Walnut shells as biosorbents can reduce iron in wastewater.	[32]
16.	Walnut Shells	Carbon	Silica particles derived from rice husk were found to be effective at adsorbing curcumin molecules. The Freundlich isotherm model is an appropriate adsorption model for this study.	[33]
17.	Rice Husk	Silica	The most suitable adsorption isotherm model is the Dubinin-Radushkevich isotherm model. The findings show that multilayer adsorption occurs for all micrometre sizes and that it involves physical interactions between the adsorbate and the adsorbent surface.	[34]
18.	Barred Fish (*Scomberomorus spp.)* Bone	Calcium Carbonate	The results revealed that adsorbents from tea waste are very promising to remove waste ions Ni and Co.	[35]
19.	Tea	Fe_2O_3	The adsorption data of the Fe_2O_3 adsorbent followed the Langmuir model and the kinetic data followed the second order. Based on the research results, Fe_2O_3 adsorbent from cherry peel waste was able to remove chromium (IV) with maximum adsorption capacities of 47.576 mg/g.	[36]
20.	Cherry Peel	Carbon	Carbon preparation of rice straw makes porous carbon particles effective and the change in porosity has a direct impact on the ability of the product to absorb molecules.	[37]

This study aimed to investigate the characteristic isotherm adsorption of carbon microparticles from jackfruit seeds to remove curcumin dyes from aqueous solutions. Jackfruit seeds were chosen because they contain lignocellulose (35-50%), hemicellulose (20-35%), and lignin (10-25%) [37]. In particular, the high lignocellulose content of jackfruit seeds when burned into carbon can be used as an adsorbent to remove dyes from waste [38]. In addition, according to the Central Statistics Agency, jackfruit production in Indonesia reached 779,859 tons in 2019, the edible portion of the jackfruit flesh ranges from 20 to 30%, and the seed portion from 5-15%. Based on the amount of jackfruit production, the jackfruit seeds that can be produced can reach 38,992 to 116,978 tons/year [39]. Hence, an understanding of converting jackfruit seed waste into carbon as an adsorbent is useful as a way to overcome environmental problems due to the increasing amount of jackfruit seed waste, especially in Indonesia. In this study, we not only focused on the synthesis and characterization of carbon but also focused on the analysis of the isotherm phenomenon of carbon microparticle adsorption from jackfruit seeds. For this reason, the phenomenon of adsorption plays an important role involved when the particles present are adsorbed on the surface. It is useful to distinguish between adsorption, where the particles stick to the surface, and desorption, which is the opposite. This research is expected to provide insight into its use as a low-cost adsorbent-derived jackfruit seed to remove organic dyes from dissolving.

2. Isotherm Adsorption Model

In this study, experimental data were fitted into various theoretical isotherm models to describe the adsorption process discussed by Ragadhita and Nandiyanto [40]. Ten parameter models: Langmuir, Freundlich, Temkin, Dubinin-Radushkevich, Fowler-Guggenheim, Hill-Deboer, Jovanovic, Harkin-Jura, Flory-Huggins, and Halsey models were used to determine the adsorption process that occurs monolayer, multilayer, or cooperatively. Figure 1(a) depicts the phenomena of the monolayer. Figure 1(b) depicts the phenomena of multilayer, and cooperative adsorption processes. An explanation of the adsorption isotherm model is provided in detail below [40, 41].

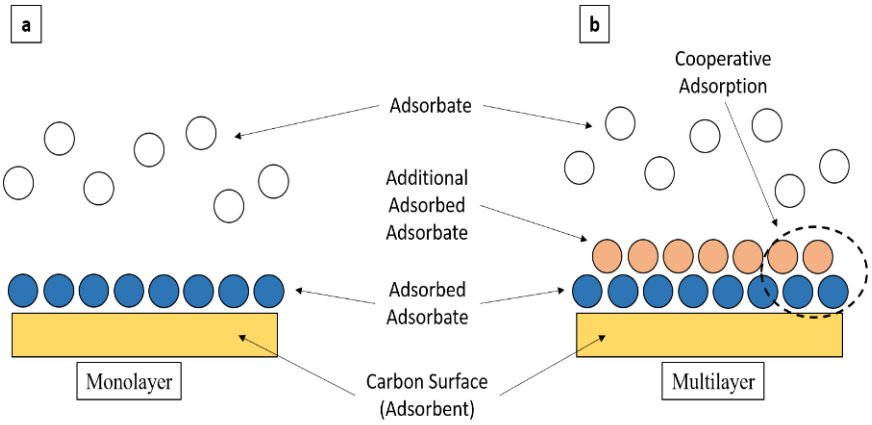

Fig. 1. Illustration of the monolayer, multilayer, and cooperative adsorption process (adapted from Nandiyanto et al. [15]).

2.1. Langmuir isotherm

Langmuir isotherm defines that the maximum adsorbent occurs due to the presence of a single layer (monolayer) of adsorbate on the surface of the adsorbent. There is an assumption based on the Langmuir isotherm namely, there is no interaction between the adsorbent and the adsorbent, there is no transmigration of the adsorbate, and the molecules adsorbed by the adsorbent occur on a fixed surface, each surface has the same energy. Equations (1) and (2) can be used to predict the Langmuir isotherm equation [15].

$$\frac{1}{Q_e} = \frac{1}{Q_{max} K_L} \frac{1}{C_e} + \frac{1}{Q_{max}} \tag{1}$$

$$R_L = \frac{1}{1 + K_L C_e} \tag{2}$$

where K_L is the Langmuir adsorption constant, Q_{max} is the maximum monolayer adsorption capacity (mg/g), and R_L is the separation factor. The description of the R_L value is following:

(i) When $R_L > 1$, Adsorption is in unfavourable condition because desorption occurs.

(ii) When $R_L = 1$, Adsorption is in linear condition (depends on the amount adsorbed and the concentration of adsorbent.

(iii) When $R_L = 0$, Adsorption said it is to be irreversible because fabulous (usually occurs in chemisorption).

(iv) When $0 < R_L < 1$, Adsorption said it is advantageous because no desorption occurs (usually occurs under conditions.

2.2. Freundlich isotherm

Freundlich isotherm assumes the adsorption site is heterogeneous with the type of physical adsorption occurring in several layers and the bond is not strong. This model implies that the energy on each surface is not the same. Equation (3) can be used to express the Freundlich isotherm model [15].

$$\log Q_e = log k_f + \frac{1}{n} \log C_e \tag{3}$$

where k_f is the Freundlich constant, *Ce* is the adsorbate concentration at equilibrium (mg/L), n is the degree of non-linearity, and $1/n$ is the adsorption strength. The express meaning of the n and $1/n$ parameters is following:

(i) If $n < 1$, it indicates the adsorption process is chemisorption

(ii) If $n = 1$, it indicates the adsorption process with the partition between two phases is unaffected by concentration

(iii) If $n > 1$, it indicates the adsorption process is chemisorption physisorption

(iv) If $1/n < 1$, it indicates the adsorption process is normal

(v) If $1/n > 1$, it indicates the adsorption process is cooperative

(vi) If $1 < 1/n < 0$, it indicates the adsorption process is a favourable adsorption (it is because there is no occurs desorption process)

(vii) If $0 < 1/n < 1$, it indicates the adsorption process that occurs on heterogeneous surfaces (where the value of 1/n is close to 0 indicating that the surface of the adsorbent is getting more heterogeneous).

2.3. Temkin isotherm

Temkin Isotherm defines that the heat of adsorption (a function of temperature) of all molecules in the layer will decrease linearly rather than logarithmically regardless of very low and large concentration values. The heat of adsorption of all molecules in the multilayer was calculated using Eq. (4) [15].

$$q_e = \beta_T(lnC_e) + (\beta_T lnA_T) \quad (4)$$

where A_T is the Temkin isotherm model's equilibrium constant and T is the Temkin isotherm. The description of the T parameter is following:

(i) If $\beta_T < 8$ kJ/mol indicates the heat of sorption is physical adsorption

(ii) If $\beta_T > 8$ kJ/mol Indicates the heat of sorption is chemical adsorption

2.4. Dubinin-Raduskevich isotherm

Dubinin-Radushkevich isotherm explains the adsorption mechanism with a Gaussian energy distribution at a heterogeneous surface. This model is that the adsorbent size is proportional to the micropore size and the adsorption equilibrium relationship for a given adsorbate-adsorbent combination can be expressed independently of temperature using the adsorption potential (ε). Equation (5) shows the Dubinin-Radushkevich model's adsorption equation.

$$lnq_e = lnq_s - \beta\varepsilon^2 \quad (5)$$

where q_s represents the theoretical saturation capacity (mg/g), and ε is the Polanyi potential associated with the conditions. Equations (6) and (7) state the Polanyi potential and the calculation of the adsorption energy.

$$\varepsilon = RT \ln\left[1 + \frac{1}{C_e}\right] \quad (6)$$

$$E = \frac{1}{\sqrt{2\beta}} \quad (7)$$

where β is sorption free energy (kJ mol^{-1}) per molecule of sorbate at the moment of its transfer to the solid surface from the bulk solution, E is the adsorption energy. The description of the E value is following:

(i) If $E < 8$ kJ/mol indicates that the adsorption energy occurs at physical adsorption

(ii) If $E > 8$ kJ/mol indicates that the adsorption energy occurs at chemical adsorption

2.5. Dubinin-Raduskevich isotherm

Fowler-Guggenheim isotherm describes the lateral interactions of the adsorbed molecules that depend on the heat of adsorption which varies positively or negatively with loading. If the interaction energy is positive with the force of attraction, the heat of adsorption increases directly with loading. Meanwhile, in the case of the energy repulsion of the adsorbed molecules, there is a reduction in loading. In Equation 8 the linear form of this model is elucidated.

$$K_{FG}C_e = \frac{\theta}{1-\theta} exp\ (\frac{2.\theta.W}{RT}) \quad (8)$$

where K_{FG} is the Fowler-Guggenheim equilibrium constant (L/m), and W is the interaction energy (kJ/mol) between the adsorbed molecules. The description of the W value is following:

(i) If W < 8 kJ/mol, it indicates that the process of attraction between the adsorbed molecule is exothermic

(ii) If W > 0 8 kJ/mol, it indicates that the process of repulsion between the adsorbed molecules for the adsorbed molecule is endothermic

(iii) If W = 0 kJ/mol, it indicates no interaction between the adsorbed molecules.

2.6. Hill-de Boer isotherm

Hill-de Boer isotherm describes mobile adsorption and lateral interactions between the adsorbed molecules which depend on the type of force between the adsorption molecules according to the model parameter values. A further explanation for the Hill-de Boer isotherm is given by Eq. (9).

$$K_1.C_e = \frac{\theta}{1-\theta} exp\ (\frac{\theta}{1-\theta} - \frac{K_2\theta}{RT}) \quad (9)$$

where K_1 (L/mg) and K_2 (kJ/mol) are the Hill-de Boer model's parameter and the energetic constant of interaction in the adsorbed molecular, respectively. The description of the K_2 value is following:

(i) If K_2 > 0 kJ/mol, it indicates that the process of attraction between the adsorbed molecule is exothermic

(ii) If K_2 < 0 kJ/mol, it indicates that the process of repulsion between the adsorbed molecules for the adsorbed molecule is endothermic.

(iii) If K_2 = 0 kJ/mol, it indicates that no interaction between the adsorbed molecules.

2.7. Jovanovic Isotherm

Jovanovic isotherm assumes the possibility of mechanical contact between the adsorbate and the adsorbent by considering the phenomena in the Langmuir model. The linear equation of the Jovanovic isotherm is shown by Eq. (10).

$$nQ_e = lnQ_{max} - K_jC_e \quad (10)$$

where K_J (l/g) is the parameter of the Jovanovic model.

2.8. Harkin-Jura isotherm

Harkins-Jura isotherm explains the multilayer adsorption process depending on the heterogeneous pore distribution. The equation of this model is expressed by Eq. (11).

$$\frac{1}{q_e^2} = \frac{B_{HJ}}{A_{HJ}} - \left(\frac{1}{A}\right) logC_e \quad (11)$$

where A_{HJ} (g^2/l) and B_{HJ} (mg^2/l) are the Harkin-Jura model parameters and the specific surface area of the adsorbent that characterizes the adsorption miracle, respectively.

2.9. Flory-Huggins Isotherm

Flory-Huggins isotherm model assumes a multilayer adsorption process that depends on the pore surface of the adsorbent. It is given in Eq. (12).

$$log\frac{\theta}{C_e} = logK_{FH} + n\log(1-\theta) \quad (12)$$

where $\theta = \left(1-\frac{C_e}{C_o}\right)$ is the degree of surface cover, n_{FH} and K_{FH} are the Flory-Huggin constants defined as the amount of adsorbate occupying the adsorption site and the adsorption equilibrium constants, respectively. To calculate the Gibbs free energy ($\Delta G°$) of spontaneous adsorption, the value of $\Delta G°$ can be calculated from the equilibrium constant (K_{FH}), as shown in Eq. (13).

$$\Delta G° = -RTlnK_{FH} \quad (13)$$

The presence of a negative value for $\Delta G°$ indicates that the adsorption process is spontaneous and temperature dependent.

2.10. Halsey isotherm

Halsey isotherm is used to evaluate adsorption with the multilayer adsorption process. Equation (14) expressed the Halsey isotherm equation.

$$Q_e = \frac{1}{n_H}lnK_H - \left(\frac{1}{n_H}\right)lnC_e \quad (14)$$

Table 2 details the curves of the data fitting results and the calculation of each adsorption isotherm parameter.

Table 2. Adsorption isotherms fitting data, calculation, and their parameters.

Isotherm Model	Linear Equation	Plotting x	Plotting y	Parameter
Langmuir	$\frac{1}{Q_e} = \frac{1}{Q_{max}K_L}\frac{1}{C_e} + \frac{1}{Q_{max}}$	$1/C_e$	$1/Q_e$	$\frac{\mathbf{1}}{\boldsymbol{Q_{max}}} = intercept$ $\boldsymbol{k_L} = \frac{\mathbf{1}}{\boldsymbol{Q_{max} \times slope}}$
Freundlich	$log\,Q_e = log\,k_f + \frac{1}{n}\,log\,C_e$	lnC_e	lnQ_e	• slope • $\ln k_f = intercept$
Temkin	$Q_e = \boldsymbol{B}_T\ \ln A_T + B_T \ln C_e$	lnC_e	Q_e	• B = slope • $\boldsymbol{B}_T\ \ln A_T$ = intercept • $B_T = \frac{RT}{B}$
Dubinin-Radushkevich	$\ln Q_e = \ln q_s - (\beta\varepsilon^2)$	ε^2	lnQ_e	• $\beta = K_{DR} = slope$ • $E = \frac{1}{\sqrt{2\times K_{DR}}}$
Flory Huggins	$log\frac{\theta}{C_e} = logK_{FH} + n\log(1-\theta)$	$log\left(\frac{\theta}{C_0}\right)$	$log(1-\theta)$	• $n_{FH} = slope$ • $k_{FH} = intercept$ • $\Delta G° = RT\ln(k_{FH})$ • $\theta = 1 - (\frac{C_e}{C_0})$
Fowler-Guggenheim	$ln\left(\frac{C_e(1-\theta)}{\theta}\right) - \frac{\theta}{1-\theta} = -lnK_{FG} + \frac{2W\theta}{RT}$	θ	$ln\left[\frac{C_e(1-\theta)}{\theta}\right]$	• $W = slope$ • $-lnK_{FG} = intercep$ • $\alpha(slope) = \frac{2W\theta}{RT}$ • $\theta = 1 - (\frac{C_e}{C_0})$

Hill-Deboer	$ln\left[\frac{C_e(1-\theta)}{\theta}\right]-\frac{\theta}{1-\theta} = -lnK_1-\frac{K_2\theta}{RT}$	θ	$ln\left[\frac{C_e(1-\theta)}{\theta}\right] -\frac{\theta}{1-\theta}$	• $-lnk_1 = intercept$ • $\alpha(slope)=\frac{k_2\theta}{RT}$ • $\theta = 1-(\frac{C_e}{C_0})$
Jovanovic	$lnq_e = lnq_{max} - K_J C_e$	C_e	lnQ_e	• $K_J = slope$ • $lnq_{max} = intercept$
Harkin-Jura	$\frac{1}{q_e^2}=\frac{B}{A}-\left(\frac{1}{A}\right)logC_e$	$logC_e$	$\frac{1}{q_e^2}$	• $A_H=\frac{1}{Slope}$ • $\frac{B_H}{A_H}=intercept$
Halsey	$lnQ_e=\frac{1}{n_H}lnK_H-\frac{1}{n}lnC_e$	lnC_e	lnQ_e	• $\frac{1}{n}=slope$ • $\frac{1}{n}lnK_H=intercept$

Furthermore, to calculate the amount that is obsessed by the unit mass of the adsorbent at equilibrium, Equation (15) is used.

$$Q_e=\frac{C_o-C_e}{m}\times V \quad (15)$$

where *Co* is the initial concentration (mg/L), *Ce* is the equilibrium concentration (mg/L), *m* is the adsorbent mass (g), and *V* is the adsorbate solution volume (L).

3. Material and Method

3.1. Materials

In this study, the raw materials used for prepared carbon particles were jackfruit (*Artocarpus heterophyllus Lam*.) seeds (purchased from Market in Bandung, Indonesia), distilled water (purchased from Sakura Medical Store, Bandung, Indonesia), and curcumin (purchased from Market in Bandung, Indonesia).

3.2. Preparation of carbon particles from jackfruit seeds

Carbon particles were prepared according to our previous study [15]. Previously, 1000 grams of jackfruit was first separated from the seeds. Then, the seeds were washed with distilled water and carbonized in an oven at 230°C for 7 hours. Furthermore, the carbonized jackfruit seeds were saw-milled for 5 minutes to get jackfruit seed powder. To determine the specific size of carbon, a sieve test analysis was performed using a sieve (PT Rumah Publication Indonesia) with sizes of 500, 250, 100, 74, and 60 μm.

3.3. Particles characterization

The morphology investigation of prepared carbon particles was analysed using Digital Microscope (BXAW-AX-BC, China). To analyse the chemical structure of the prepared carbon particles, we performed characterization using Fourier Transform Infrared (FTIR-4600, Jasco Corp., Japan).

3.4. Batch adsorption experimental

In this study, the adsorption procedure using the batch method was carried out by adding 0.05 g of carbon particles (as an adsorbent) into 140 mL of turmeric solution (as a dye molecule model) with specific concentrations of 100, 80, 60, 40, and 20 ppm. Then, the turmeric solution containing the adsorbent was stirred at a speed of

1000 rpm for 120 minutes at room conditions with a constant pH. Furthermore, the solution was taken from the mixed solution and filtered through a nylon membrane syringe filter with a pore size of 0.22 m. After that, the concentration of the solution was tested using a Visible Spectroscopy (Model 7205; JENWAY; Cole-Parner; US) tuned to a maximum wavelength in the range of 280 to 500 nm.

The data from the adsorption results were graphed and normalized. To determine the concentration of curcumin, the maximum absorption peak was calculated using Beer's Law. Furthermore, the concentration data were plotted and compared with 10 standard adsorption isotherm models, namely Langmuir, Freundlich, Temkin, Dubinin-Radushkevich, Fowler-Guggenheim, Hill-Deboer, Jovanovic, Harkin-Jura, Flory-Huggins, and Halsey.

4. Results and Discussion

4.1. Physical properties of carbon particles

Microscopic images of carbon particles from jackfruit seeds are shown in Figs. 2(a) and (b). Carbon particles are agglomerated and inhomogeneous. Ferret analysis on the particle size distribution of carbon is shown in Fig. 2(c). This analysis is useful to help determine the size of the dominating particles of carbon. Carbon has a mean size of 280 μm and a standard deviation of 26 μm.

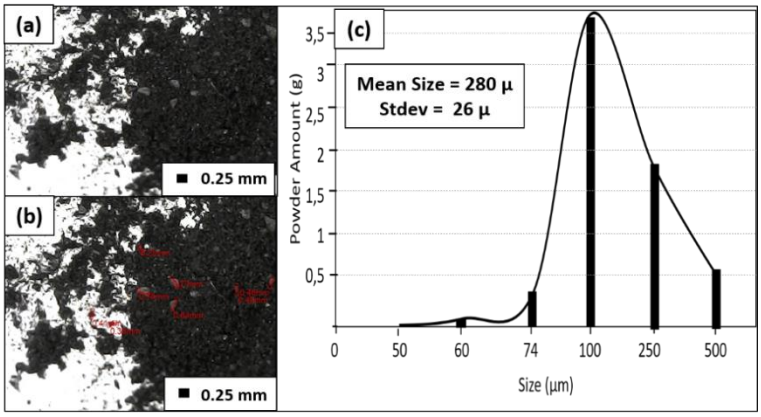

Fig. 2. (a) and (b). Microscope images of carbon particles, and (c) particles size ferret analysis of carbon particles

4.2. Characteristic adsorption of carbon particles

Experimental data was used to test the adsorption characteristics of carbon particles from jackfruit seeds which were analysed for compatibility with the ten standard adsorption isotherm models shown in Fig. 4. Based on the results of fitting the adsorption isotherm model data, four models were found that were perfectly fit, namely Langmuir, Freundlich, Jovanic, and Halsey isotherms model with a correlation coefficient value (R^2 = > 0.85). More detail about the correlation coefficient and adsorption parameters are presented in Table 3.

Figure 3(a) is the result of plotting Langmuir model data which was analysed using equations (1) and (2). The correlation coefficient value of adsorption data in

the Langmuir model is R^2 = 0.9159 with a maximum adsorption capacity (Q_{max}) is 909.9090 mg/g. The value of the R_L parameter is 0.929 – 0.984 (see Table 3). Based on the value of the correlation coefficient (R^2) and the value of the R_L parameter indicates that the adsorption process is very favourable to occur on the monolayer surface [15].

Figure 3(b) describes the results of plotting the Freundlich model based on equation 3. The R^2, n, $1/n$ values of the Freundlich isotherms are 0.8509, respectively; 1.125; and 0.8888 (see Table 3). Based on the Freundlich isotherm parameter values are $n > 1$ and $0 < 1/n <$ inform that the adsorption process is physical (physisorption) at a favourable [15].

Figure 3(c) is the curve of the Temkin plotting isotherm adsorption model studied from equation 4. The Temkin model assumes that the distribution of all molecules having uniform energy on the surface of the adsorbent has a linearly decreasing heat of adsorption. From the analysis of the Temkin isotherm model, the value of R^2 = 0.7956 indicates that the adsorbate distribution occurs on a homogeneous surface. Parameter values A_T and β_T are 2.222 L/g and 0.0798 J/mol (see Table 3) which indicates that the adsorption process is physical adsorption [15].

Figure 3(d) is the result of the Dubinin-Raduskevich model adsorption isotherm analysis. The value of the relation coefficient (R^2) and the E parameter of the Dubinin-Raduskevich model are 0.7494 and 0.256 kJ/mol (see Table 3). Based on the analysis of the Dubinin-Raduskevich isotherm model, indicates that there is a physical adsorption process on a uniform surface [15].

Figure 3(e) is an analysis of the calculation of the Fowler Guggenheim isotherm model. The value of the relation coefficient (R^2) of the Fowler Guggenheim model is 0.31 and the value of the W parameter of the Fowler Guggenheim model is -63.145.1450 (see Table 3) which informs us there is a repulsive interaction between adsorbates on a single surface [40].

Figure 3(f) represents the calculation results of the Hill-de Boer model graph. The value of the relation coefficient (R^2) of the Hill-de Boer model is 0.3917 with the value of the K_2 parameter - 82,300,849 (see Table 3). Based on the results of the analysis of the Hill-de Boer model, it shows the interactions occurring between the adsorbate repel on a homogeneous surface [40].

Figure 3(g) shows the results of the Jovanovic model adsorption graph. The Jovanovic model has a relation coefficient value (R^2) is 0.9383 and the value of the Jovanic K_J isotherm constant is 0.1286 L/mg with the maximum adsorption value (Q_{max}) is 10,877 mg/g (see Table 3). Based on the results of the relatively small Qmax analysis and the R^2 value in the Jovanovic model, it was revealed that the interaction between the adsorbate was weak and the adsorption process that occurred in the monolayer [41].

Figure 3(h) depicts the results of the analysis of the Harkin-Jura adsorption model. The isotherm constant value of the Harkin-Jura model (A_{HJ}) is 0.0188, and the value of the adsorption surface area (B_{HJ}) is 1.3940 (see Table 3). Based on the value of the relation coefficient (R^2) is 0.3879 assuming that the adsorption process that occurs in the monolayer [41].

Figure 3(i) is the interpretation of the adsorption data of the Flory-Huggins isotherm model. The value of the correlation coefficient (R^2) is 0.1762 which

indicates the monolayer adsorption process. The parameter value of n_{FH} is -0.037 assuming there is a free interaction between the adsorbate molecule and the surface of the adsorbent (see Table 3). This model also informs the free energy with a positive value indicating that the adsorption process that occurs is non-spontaneous [41].

Figure 3(j) interprets the calculation of the Halsey adsorption model. The values of Halsey's constant n and K_H are 1.1251 and 1.3544 (see Table 3). Based on the parameter value of the correlation coefficient (R^2) is 0.8509 assuming the adsorption process that occurs is monolayer [41]

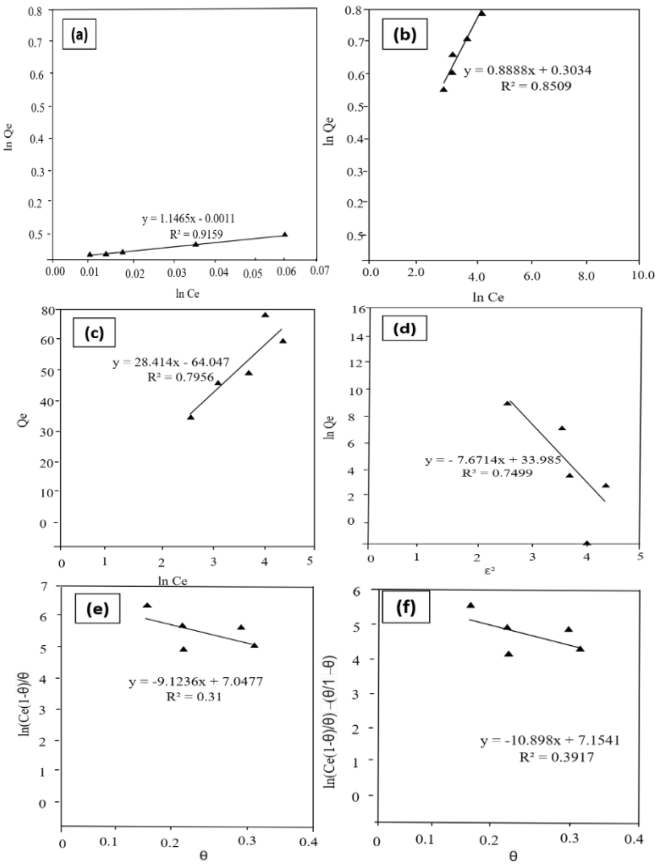

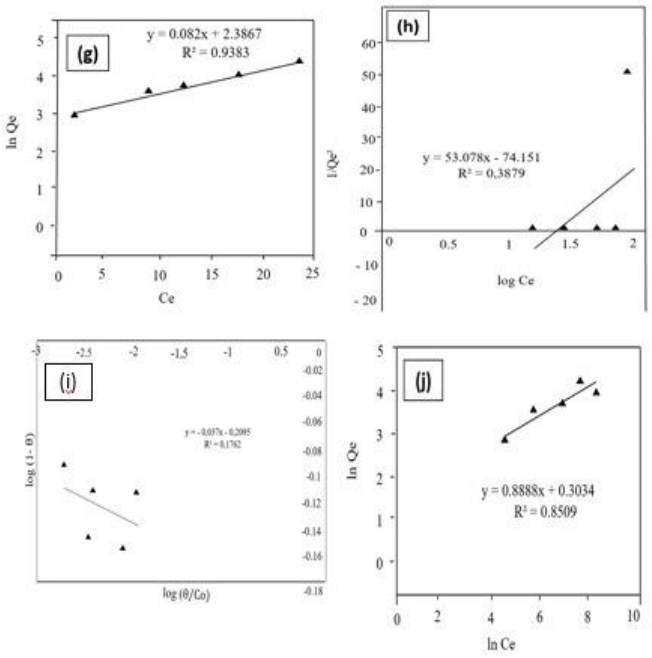

Fig. 3. Data fitting with isotherm models (a) Langmuir; (b) Freundlich; (c) Temkin; (d) Dubinin-Radushkevich; (e) Fowler-Guggenheim; (f) Hill-Deboer; (g) Jovanovic; (h) Harkin-Jura; (i) Flory-Huggins; and (j). Halsey.

Table 3. Detailed data of adsorption isotherm parameters.

Model	Parameter	Value	Note
Langmuir	Q_{max} (mg/g)	0.9159	The existence of a monolayer on the adsorbent's surface ($R^2 > 0.90$).
	K_L (L/mg)	9.5944×10^{-4}	The small value Langmuir constant indicates a weak interaction between adsorbate and adsorbent
	R_L	0.929 – 0.984	Favourable adsorption ($0 < R_L < 1$)
	R^2	0.9159	The existence of a monolayer on the adsorbent's surface ($R^2 > 0.90$).
Freundlich	K_F (mg/g)	2.4322	Adsorbent adsorption capacity
	1/n	0.8888	Adsorption process favourable ($0 < 1/n < 1$)
	n	1.125	Physisorption ($n > 1$)
	R^2	0.8509	The presence of a monolayer on the adsorbent's surface ($R^2 < 0.90$)
Temkin	A_T (L/g)	2.222	Temkin equilibrium binding constant
	β_T (J/mol)	0.0798	Physical adsorption ($\beta_T > 8$ kJ/mol)
	R^2	0.7956	Adsorbate distribution on the adsorbent surface is uniform ($R^2 < 0.90$)
	Qs (mg/g)	1.406	Capacity adsorption of adsorbent

Model	Parameter	Value	Note
Dubinin-Radushkevich	B (mol^2/kJ^2)	-7.6714	Constant of the Dubinin-Radushkevich isotherm
	E (kJ/mol)	0.256	Physisorption (E < 8 kJ/mol)
	R^2	0.7494	Micropores are present on the adsorbent surface (R^2 > 0.90).
Fowler-Guggenheim	R^2	0.31	The presence of a monolayer on the adsorbent's surface (R^2 < 0.90).
	W (kJ/mol)	-63,145.1450	Interaction between adsorbed molecules is repulsive (W < 0 kJ/mol)
	K_{FG} (L/mg)	8.694×10^{-4}	Fowler-Guggenheim isotherm constant
Hill-Deboer	R^2	0.3917	The presence of a monolayer on the adsorbent's surface (R^2 < 0.90)
	K_1 (L/mg)	7.814×10^{-4}	Hill-Deboer isotherm constant
	K_2 (kJ/mol)	- 82,300.849	Interaction between adsorbed molecules repulsive is endothermic (K_2 < 0 kJ/mol)
Jovanovic	R^2	0.9383	The presence of a monolayer on the adsorbent's surface (R^2 > 0.90)
	K_J (L/mg)	0.082	Jovanovic isotherm constant
	Q_{max} (mg/g)	10.877	Maximum uptake of adsorbate
Harkin-Jura	R^2	0.3879	No existence on multilayer the surface of adsorbent (R^2 < 0.90)
	A_{HJ}	0.0188	Harkin-Jura isotherm constant
	B_{HJ}	1.3940	Related to the surface area of the adsorbent
Flory-Huggins	R^2	0.1762	The presence of a monolayer on the adsorbent's surface (R^2 < 0.90)
	n_{FH}	-0,037	The adsorbate takes up more than one active adsorbent zone (n_{FH} < 1)
	K_{FH} (L/mg)	1.6199	Flory-Huggins isotherm constant
	$\Delta G°$ (kJ/mol)	3.676	Non-spontaneously adsorption ($\Delta G°$ > 0)
Halsey	R^2	0.8509	The presence of a monolayer on the adsorbent's surface (R^2 < 0.90)
	n	1.1251	Halsey isotherm constant
	K_H	1.3544	Halsey isotherm constant

In the previous explanation, it has been explained clearly about the adsorption isotherm used to explain the mechanism of the adsorption process. The value of the relation coefficient (R^2) was used to evaluate the suitability of the adsorption isotherm model. If the value of R^2 is closer to the value of 1, the more suitable the adsorption isotherm model is. The order of suitability of the adsorption isotherm model of carbon from jackfruit seeds to remove dye from curcumin is as follows: (1) Jovanic (R^2 = 0.9383); (2) Langmuir (R^2 = 0.9159); (3) Freundlich (R^2 = 0.8509); (4) Halsey (R^2 = 0.8509); (5) Temkin (R^2 = 0.7956) (6) Dubinin-Radushkevich (R^2 = 0.7494); (7) Hill-Deboer (R^2 = 0.3917); (8) Harkin-Jura (R^2 = 0.9585); (9) Fowler-Guggenheim (R^2 = 0.31); (10) Flory-Huggins (R^2 = 0.1762) [15, 18].

Based on the findings, the correlation coefficient (R^2) for the adsorption of curcumin dye molecules on the adsorbent prepared was the highest (closer to) the Jovanic isotherm model. The well-fitted Jovanic isotherm shows a homogeneous surface interaction of the curcumin dye molecule on the carbon adsorbent which is a monolayer adsorption system. These findings were confirmed by the Langmuir isotherm model with a high correlation value ($R^2 > 0.90$) indicating that in this experiment the adsorption process occurred on the monolayer surface with a maximum adsorption capacity of 909.9090 mg/g to remove curcumin dye molecules.

The adsorption process follows monolayer adsorption because the results of the analysis of the adsorption process most closely match the Jovanic isotherm model. The adsorption of carbon from jackfruit seeds for curcumin dye molecules followed physisorption interactions which indicated that the adsorbent was homogeneous with micropores (confirmed by the Temkin and Dubinin-Radushkevich model) through the interaction between the adsorbent and weak adsorbate. This implies that the adsorbate can move freely from one part of the surface to another through Van der Waals forces resulting in a slight heat generation than the sublimation of the adsorbate. Meanwhile, the interaction between the adsorbates was repulsive on a homogeneous surface (monolayer) is endothermic (as shown by Harkin-Jura, Halsey, and Hill-de Boer). Based on the findings, overall the adsorption process was normal (confirmed by the Freundlich isotherm), non-spontaneous (as shown by the Flory-Huggins isotherm), and favourable (confirmed by the Freundlich isotherm).

5. Conclusion

The fabrication of environmentally friendly jackfruit seeds carbon as an adsorbent has been successful to remove curcumin dye. In addition, experimental adsorption isotherm data were also stored. Comparatively, based on the correlation coefficient (R^2) obtained from the adsorption process coupled to the isotherm model in the following order: Jovanic ($R^2 = 0.9383$) < Langmuir ($R^2 = 0.9159$) < Freundlich ($R^2 = 0.8509$) < Halsey ($R^2 = 0.8509$). The adsorption isotherm modeling showed that the dye absorption occurred on the monolayer surface which proceeded normally with a maximum adsorption capacity of 909.9090 mg/g and a large saturation coverage at the occupancy of these sites. Furthermore, the average adsorption energy, E (kJ/mol) molecular and free energy of adsorption $\Delta G°$ (kJ/mol) approach from the Dubinin-Radushkevich and Flory-Huggins model which shows a physisorption mechanism of attraction between adsorbates non-repelling, and spontaneous. This study reveals that carbon from jackfruit seeds is a better low-cost, environmentally friendly adsorbent.

References

1. Kavithayeni, V.; Geetha, K.; and Akash Prabhu, S. (2019). A review on dye reduction mechanism using nano adsorbents in wastewater. *Adsorption*, 43(652), 44, 332-339.
2. Verma, R.K.; Sankhla, M.S.; Rathod, N.V.; Sonone, S.S.; Parihar, K.; and Singh, G.K. (2021). Eradication of fatal textile industrial dyes by wastewater treatment. *Biointerface Research Applied Chemistry*, 12(1), 567-587.
3. Kaykhaii, M.; Sasani, M.; and Marghzari, S. (2018). Removal of dyes from the environment by adsorption process. *Chemistry Materials Engineering*, 6(2), 31-35.

4. Natarajan, S.; Bajaj, H.C.; and Tayade, R.J. (2018). Recent advances based on the synergetic effect of adsorption for removal of dyes from waste water using photocatalytic process. *Journal of Environmental Sciences*, 65, 201-222.
5. Kadhom, M.; Albayati, N.; Alalwan, H.; and Al-Furaiji, M. (2020). Removal of dyes by agricultural waste. *Sustainable Chemistry and Pharmacy*, 16, 100259.
6. Katheresan, V.; Kansedo, J.; and Lau, S.Y. (2018). Efficiency of various recent wastewater dye removal methods: A review. *Journal of Environmental Chemical Engineering*, 6(4), 4676-4697.
7. Moradi, O.; and Sharma, G. (2021). Emerging novel polymeric adsorbents for removing dyes from wastewater: A comprehensive review and comparison with other adsorbents. *Environmental Research*, 201, 111534.
8. Cai, Z.; Sun, Y.; Liu, W.; Pan, F.; Sun, P.; and Fu, J. (2017). An overview of nanomaterials applied for removing dyes from wastewater. *Environmental Science and Pollution Research*, 24(19), 15882-15904.
9. Othmani, A.; Magdouli, S.; Kumar, P.S.; Kapoor, A.; Chellam, P.V.; and Gökkuş, Ö. (2022). Agricultural waste materials for adsorptive removal of phenols, chromium (VI) and cadmium (II) from wastewater: A review. *Environmental Research*, 204, 111916.
10. Xu, H.; Zhang, Y.; Jiang, Q.; Reddy, N.; and Yang, Y. (2013). Biodegradable hollow zein nanoparticles for removal of reactive dyes from wastewater. *Journal of environmental management*, 125, 33-40.
11. Bhanvase, B.A.; Veer, A.; Shirsath, S.R.; and Sonawane, S.H. (2019). Ultrasound assisted preparation, characterization and adsorption study of ternary chitosan-ZnO-TiO_2 nanocomposite: Advantage over conventional method. *Ultrasonics Sonochemistry*, 52, 120-130.
12. Zhou, S.; Zhang, D.; Wang, H.; and Li, X. (2019). A modified BET equation to investigate supercritical methane adsorption mechanisms in shale. *Marine and Petroleum Geology*, 105, 284-292.
13. Moosavi, S.; Lai, C.W.; Gan, S.; Zamiri, G.; Akbarzadeh Pivehzhani, O.; and Johan, M.R. (2020). Application of efficient magnetic particles and activated carbon for dye removal from wastewater. *American Chemical Society Omega*, 5(33), 20684-20697.
14. Afroze, S.; and Sen, T.K. (2018). A review on heavy metal ions and dye adsorption from water by agricultural solid waste adsorbents. *Water, Air, & Soil Pollution*, 229(7), 1-50.
15. Nandiyanto, A.B.D.; Maryanti, R.; Fiandini, M.; Ragadhita, R.; Usdiyana, D.; Anggraeni, S.; and Al-Obaidi, A.S.M. (2020). Synthesis of carbon microparticles from red dragon fruit (*Hylocereus undatus*) peel waste and their adsorption isotherm characteristics. *Molekul*, 15(3), 199-209.
16. Song, S.; Wang, Z.A.; Gonneea, M.E.; Kroeger, K.D.; Chu, S.N.; Li, D.; and Liang, H. (2020). An important biogeochemical link between organic and inorganic carbon cycling: Effects of organic alkalinity on carbonate chemistry in coastal waters influenced by intertidal salt marshes. *Geochimica et Cosmochimica Acta*, 275, 123-139.
17. Dai, Y.; Sun, Q.; Wang, W.; Lu, L.; Liu, M.; Li, J.; and Zhang, Y. (2018). Utilizations of agricultural waste as adsorbent for the removal of contaminants: A review. *Chemosphere*, 211, 235-253.

18. Fiandini, M.; Ragadhita, R.; Nandiyanto, A.B.D.; and Nugraha, W.C. (2020). Adsorption characteristics of submicron porous carbon particles prepared from rice husk. *Journal of Engineering Science and Technology*, 15(1), 022-031.
19. Nandiyanto, A.B.D.; Girsang, G.C.S.; Maryanti, R.; Ragadhita, R.; Anggraeni, S.; Fauzi, F.M.; and Al-Obaidi, A.S.M. (2020). Isotherm adsorption characteristics of carbon microparticles prepared from pineapple peel waste. *Communications in Science and Technology*, 5(1), 31-39.
20. Nandiyanto, A.B.D.; Azizah, N.N.; and Rahmadianti, S. (2021). Isotherm study of banana stem waste adsorbents to reduce the concentration of textile dying waste. *Journal of Engineering Research*, 9(special issue), 1-15.
21. Nandiyanto, A.B.D.; Putra, Z.A.; Andika, R.; Bilad, M.R.; Kurniawan, T.; Zulhijah, R.; and Hamidah, I. (2017). Porous activated carbon particles from rice straw waste and their adsorption properties. *Journal of Engineering Science and Technology*, 12(8), 1-11.
22. Nandiyanto, A.B.D.; Hofifah, S.N.; Inayah, H.T.; Putri, S.R.; Apriliani, S.S.; Anggraeni, S.; and Rahmat, A. (2021). Adsorption isotherm of carbon microparticles prepared from pumpkin (*Cucurbita maxima*) seeds for dye removal. *Iraqi Journal of Science*, 62(5), 1404-1414.
23. Nandiyanto, A.B.D.; Arinalhaq, Z.F.; Rahmadianti, S.; Dewi, M.W.; Rizky, Y.P.C.; Maulidina, A.; Anggraeni, S.; Bilad, M.R.; and Yunas, J. (2020). Curcumin adsorption on carbon microparticles: synthesis from soursop (*Annona muricata L.)* peel waste, adsorption isotherms and thermodynamic and adsorption mechanism. *International Journal of Nanoelectronics & Material*s, 13(spesial issue), 173-192.
24. Jaishankar, M.; Mathew, B.B.; Shah, M.S.; and Gowda, K.R.S. (2014). Biosorption of few heavy metal ions using agricultural wastes. *Journal of Environment Pollution and Human Health*, 2(1), 1-6.
25. Feng, C.; Zhang, S.; Wang, Y.; Wang, G.; Pan, X.; Zhong, Q.; and Yao, P. (2020). Synchronous removal of ammonium and phosphate from swine wastewater by two agricultural wastebased adsorbents: Performance and mechanisms. *Bioresource Technology*, 307, 123231.
26. Stavrinou, A.; Aggelopoulos, C.A.; and Tsakiroglou, C.D. (2018). Exploring the adsorption mechanisms of cationic and anionic dyes onto agricultural waste peels of banana, cucumber and potato: Adsorption kinetics and equilibrium isotherms as a tool. *Journal of Environmental Chemical Engineering*, 6(6), 6958-6970.
27. Bharti, S.K.; and Kumar, N. (2018). Kinetic study of lead (Pb^{2+}) removal from battery manufacturing wastewater using bagasse biochar as biosorbent. *Applied Water Science*, 8(4), 1-13.
28. Vigneshwaran, S.; Sirajudheen, P.; Karthikeyan, P.; and Meenakshi, S. (2021). Fabrication of sulfur-doped biochar derived from tapioca peel waste with superior adsorption performance for the removal of malachite green and rhodamine b dyes. *Surfaces and Interfaces*, 23, 100920.
29. Gayathri, R.; Gopinath, K.P.; and Kumar, P.S. (2021). Adsorptive separation of toxic metals from aquatic environment using agro waste biochar: Application in electroplating industrial wastewater. *Chemosphere*, 262, 128031.

30. Sujatha, S.; and Sivarethinamohan, R. (2021). Application of response surface methodology to optimize lead (II) ion adsorption by activated carbon fabricated from de oiled soya. *Desalin. Water Treat,* 226, 242-250.
31. Asadi-Sangachini, Z.; Galangash, M.M.; Younesi, H.; and Nowrouzi, M. (2019). The feasibility of cost-effective manufacturing activated carbon derived from walnut shells for large-scale CO_2 capture. *Environmental Science and Pollution Research*, 26(26), 26542-26552.
32. Ragadhita, R.; Nandiyanto, A.B.D.; Nugraha, W.C.; and Mudzakir, A. (2019). Adsorption isotherm of mesopore-free submicron silica particles from rice husk. *Journal of Engineering Science and Technolo*gy, 14(4), 2052-2062.
33. Nandiyanto, A.B.D.; Erlangga, T.M.S.; Mufidah, G.; Anggraeni, S.; Bilad, R.; and Yunas, J. (2020). Adsorption isotherm characteristics of calcium carbonate microparticles obtained from barred fish (*Scomberomorus spp*.) bone using two-parameter multilayer adsorption models. *International Journal of Nanoelectronics & Materials*, 13(special issue), 45-57.
34. Shirvanimoghaddam, K.; Czech, B.; Tyszczuk-Rotko, K.; Kończak, M.; Fakhrhoseini, S.M.; Yadav, R.; and Naebe, M. (2021). Sustainable synthesis of rose flower-like magnetic biochar from tea waste for environmental applications. *Journal of Advanced Research*, 34, 13-27.
35. Altun, T.; and Ecevit, H. (2020). Cr (VI) removal using Fe_2O_3-chitosan-cherry kernel shell pyrolytic charcoal composite beads. *Environmental Engineering Research*, 25(3), 426-438.
36. Baloga, H.; Walanda, D.K.; and Hamzah, B. (2019). Pembuatan arang dari kulit nangka (*Artocarpus heterophyllus*) sebagai adsorben terhadap kadmium dan nikel terlarut. *Jurnal Akademika Kimia*, 8(1), 28-33.
37. Sunarsih, S.; and Dahani, W. (2018). Studi adsorpsi karbon aktif limbah kulit buah nangka terhadap rhodamin b. *Jurnal Teknologi*, 11(1), 46-53.
38. Miah, R.A.; Alam, M.J.; Khatun, A.; Suhag, M.H.; and Kayes, M.N. (2022). The decolorization and phytotoxic efficiency of jackfruit seed on a textile dye novacron blue. *Journal of Engineering Advancements*, 3(1), 6-11.
39. Handayani, N. (2016). Pemanfaatan limbah nangka sebagai penganekaragaman makanan. *Warta Dharmawangsa*, (47), 1-12.
40. Ragadhita, R.; and Nandiyanto, A.B.D. (2021). How to calculate adsorption isotherms of particles using two-parameter monolayer adsorption models and equations. *Indonesian Journal of Science and Technology*, 6(1), 205-234.
41. Nandiyanto, A.B.D.; Ragadhita, R.; and Yunas, J. (2020). Adsorption isotherm of densed monoclinic tungsten trioxide nanoparticles. *Sains Malaysiana*, 49(12), 2881-2890.